THE INTERACTION OF STELLAR HIGH ENERGY RADIATION WITH HYDROGEN RICH PLANETARY ATMOSPHERES

Cesare Cecchi-Pestellini

INAF OAC Osservatorio Astronomico di Cagliari

EXOPLANETS

planets beyond our Solar System, orbiting a star other than our Sun

first (firmly-established) discovered planets orbiting a pulsar in 1992
(PSR 1257+12; Wolszczan & Frail 1992)

the first definitive detection of an exoplanet orbiting an ordinary main-sequence star (51 Pegasi) was in 1995 (Mayor & Queloz 1995)

as of May 2009, 347 (293) exoplanets are listed in the
Extrasolar Planets Encyclopaedia (http://exoplanet.eu/)

most exoplanets are massive gas giant Jupiter-like planets:
selection effect due to limitations in detection technology

HOT JUPITERS

mass close (or to exceeds that) of Jupiter

unlike in the Solar System, where Jupiter orbits at 5 AU,
the planets orbit within ≈ 0.05 AU of their parent stars

- much greater chance of transiting their star than planets of the same mass in larger orbits
- migration to their present positions because there would not have been enough material so close to the star for a planet of that mass to have formed in situ.
- low eccentricities: orbits have been circularized, or are being circularized, by the process of libration
- synchronization of rotation and orbital periods, so it always presents the same face to its parent star - the planet is tidally-locked to the star
- **super levels of irradiation: lower density than they would otherwise be & mass loss**

HOT JUPITERS

mass close (or to exceeds that) of Jupiter

unlike in the Solar System, where Jupiter orbits at 5 AU, the planets orbit within ≈ 0.05 AU of their parent stars

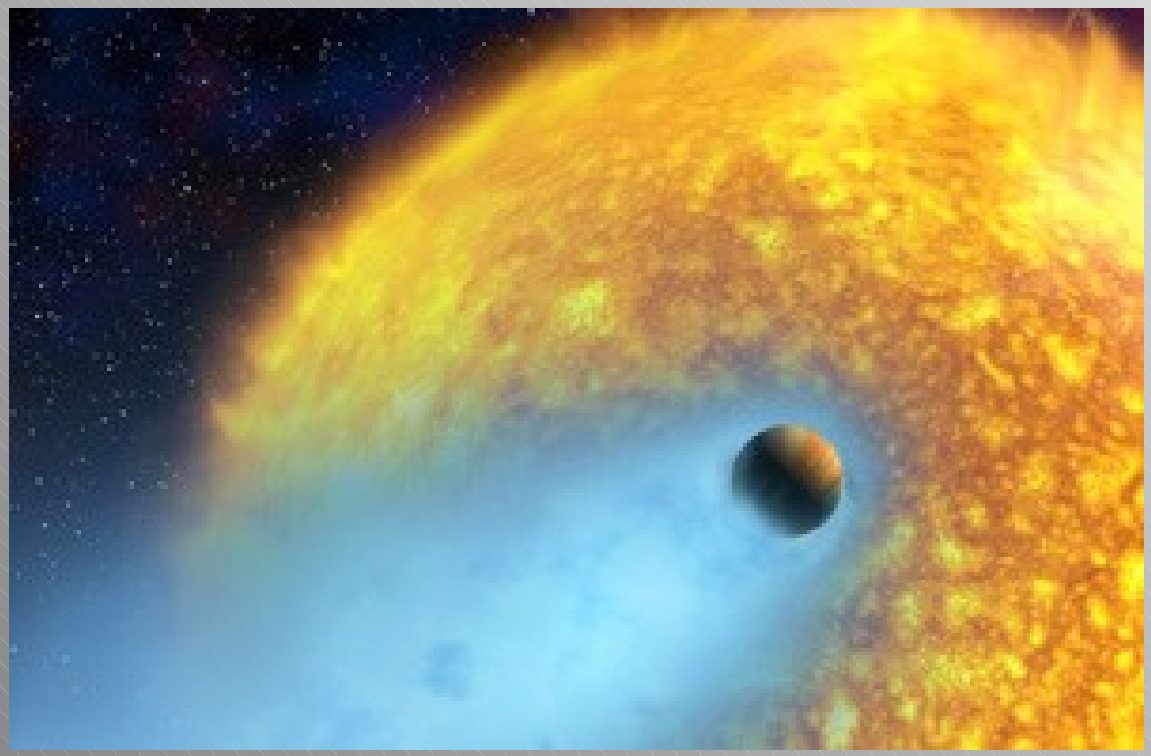

EXTREME EVENTS

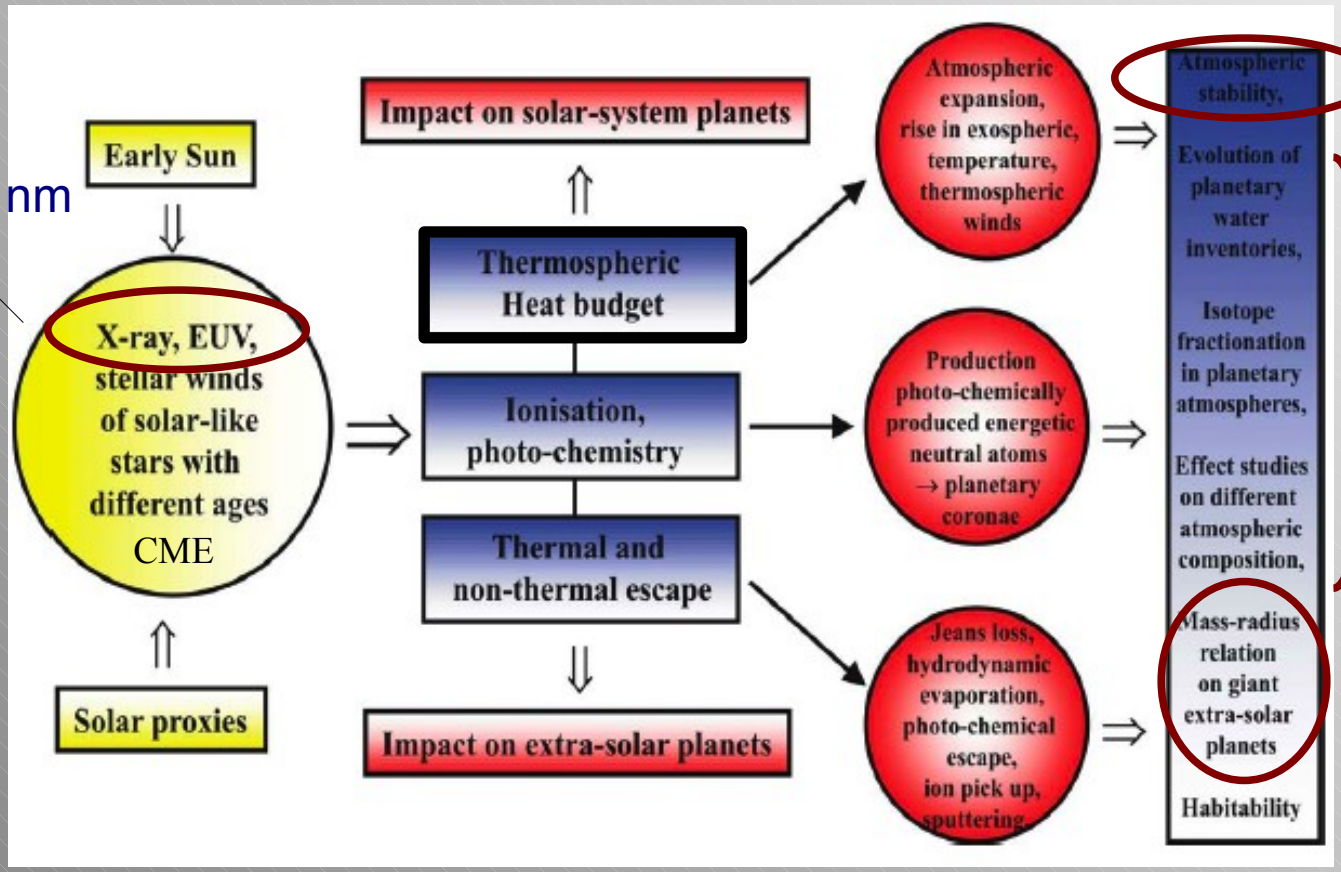

the evolution of the spectral irradiances (X-rays, EUV) of solar-type stars of different ages may be used as a proxy for reconstructing the history of the Sun's radiation

SOLAR PROXIES

young solar type stars emit X-rays at a level three to four orders of magnitude higher than the present-day Sun during both

- pre-main sequence phase when the emission is dominated by intense daily or weekly flares (Feigelson et al. 2003; Favata et al. 2005)
- the first phases of the main sequence when a solar-like star has an X-ray luminosity in the range 10^29 - 10^30 ergs/s (Micela 2002)

such an intense illumination must have affected the disk and the process of planetary formation during the pre main-sequence phase, and, subsequently when the star reached the main sequence, the evolution of planetary atmospheres

evolution of a planetary atmosphere can only be understood within the context of its own evolving stellar radiation environment

SOLAR PROXIES

bandpass

0.1 - 1 keV

1 - 10 keV

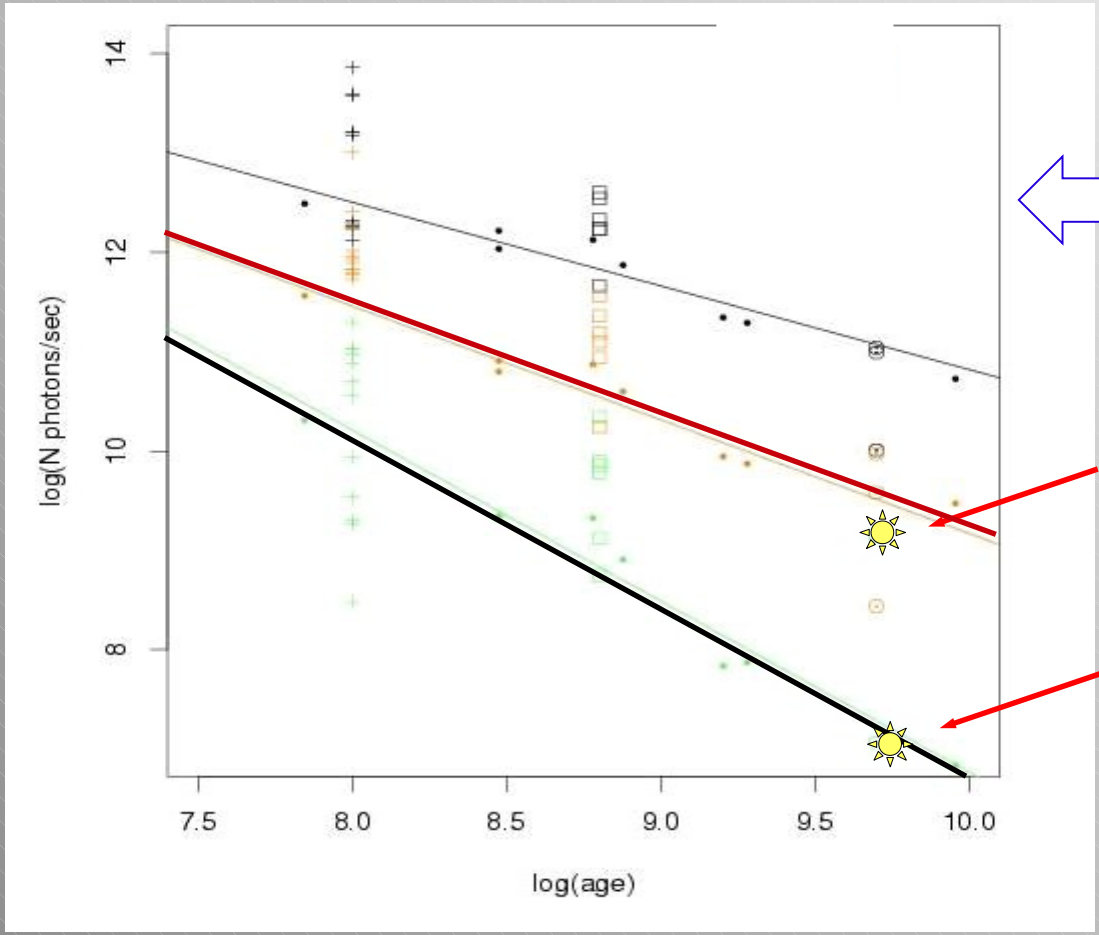

1 AU

Sun today @ max

Sun today @ min

Micela 2002

coronal temperature decreases with age

MOTIVATIONS & GOALS

- observations: hydrogen escaping hydrodynamically
- interpretation: which is the mass loss rate? 10^{12} g/s $\Rightarrow$ $\leq 10^{10}$ g/s
- conversion of absorbed stellar XUV flux into powering escape
- relative roles of EUV and X-rays in an hydrogen-rich atmosphere
- the sun at different ages

MODELING

the flux of stellar XUV photons incident upon an hydrogen-rich cloud photo-ionizes the ambient gas producing a cascade of high energy photo-electrons which deposit their energy into the gas

in a partially neutral medium, photo-electrons ionize, excite, and dissociate atomic and molecular species, as well as heat the gas through Coulomb collisions

the interaction of XUV radiation with gas clouds occurs in many astrophysical environments (e.g. AGN)

a unique feature of XUV irradiation is that all relevant processes are dominated by secondary ionizations generated by primary photoelectrons

a consequence of the large primary photoelectron energies

MODELING

radiative transfer of stellar radiation in a
H-rich planet atmosphere determines the local radiation flux,
that in turn controls

thermodynamics and chemistry of the nebular phase

dynamical feedback

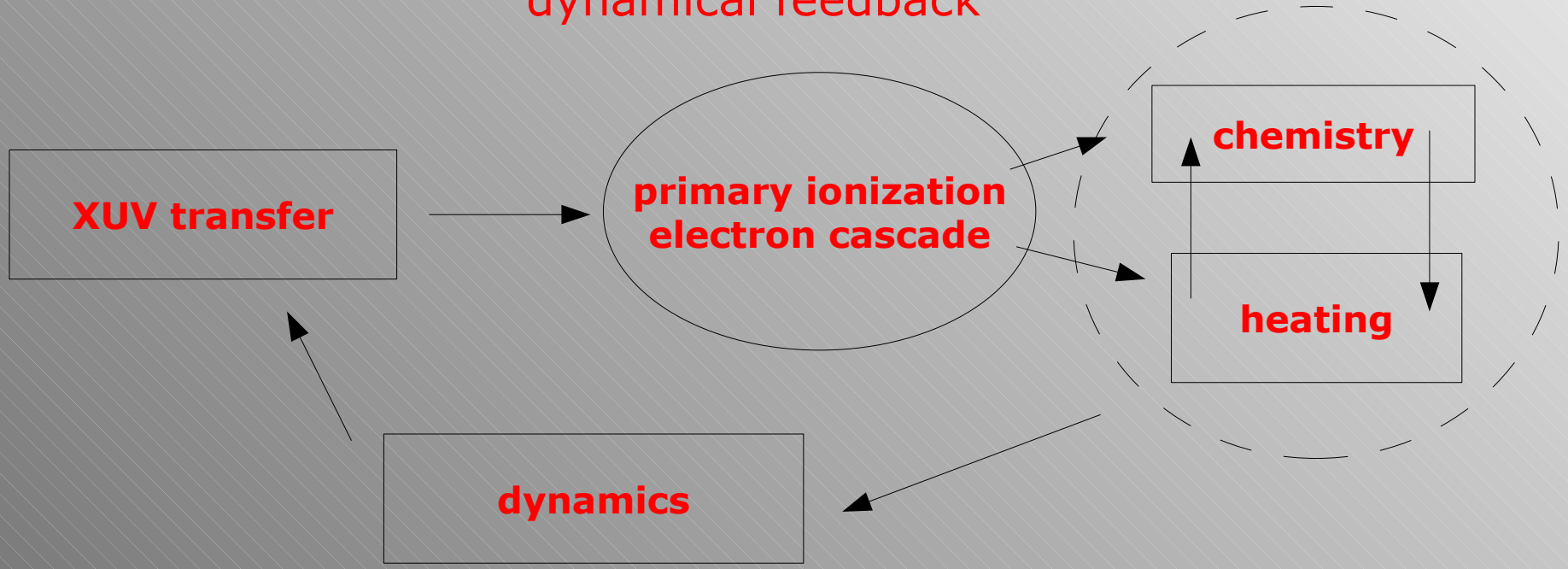

RADIATIVE TRANSFER

- plane parallel geometry
- normally incident X-ray flux
- solar composition

photo-ionization cross-sections

$$\sigma_{\rm pa}(E) = \sum_i f_i \, \sigma_i(E)$$

H,He,He^+,H_2

heavy elements

$$\tau_X(z) = \left(\sigma_{\rm pa} + \sigma_C\right) \times [N_{\rm H}(\Delta z) - N_{\rm H}(z)]$$

heavy elements in molecules
σ(XYZ) = σ(X)+σ(Y)+σ(Z)
+ (E)UV cross-sections

Compton ionization cross sections
(non relativistic) H,He,H_2

random walk technique ←

ENERGETIC PHOTO-ELECTRONS

energy degradation is characterized by

(i) the energy loss function

$$L(E) = (2m_e E/M)\sigma_{\mathrm{mt}}(E) + \frac{1}{n_M v_e}\frac{dE}{dt} + \sum_n \sigma_n(E)\Delta E_n + \sum_n \int_0^{(E-I_n)/2} (I_n + \epsilon)\frac{d\sigma_n^i}{d\epsilon}(E, \epsilon)\, d\epsilon \,,$$

(ii) mean energy for ion

$$W = E/N_{\mathrm{ion}}(E)$$

$$\frac{1}{n}\frac{dE}{dx} = -L(E) \,.$$

the energy deposition pipeline

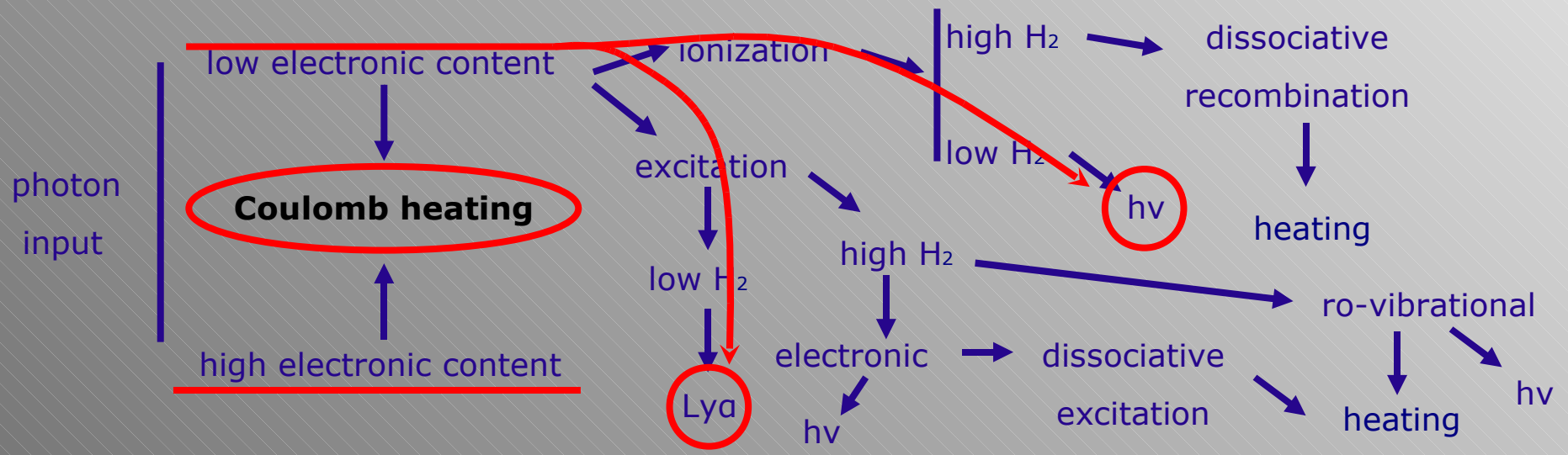

THE METHOD

Calculations performed following the history of an electron with energy E (Monte Carlo technique)

steps

- discrete set of energy bins $\{E_i\}$ such that $(E_i - E_{i-1}) <$ least energetic inelastic process contributing to the energy loss at E_i
- probabilities that any bin is emptied by exc, diss, ion, elastic collisions are computed from the cross-sections
- each subsequent bin is emptied in turn until no further inelastic scattering is energetically possible
- the energy remaining is taken up as heat

the rate at which each excited or ionized state is populated is recorded to yield the total number of excitation, ionization, and dissociation events

INPUT DATA: CROSS-SECTIONS

PHOTO-IONIZATION

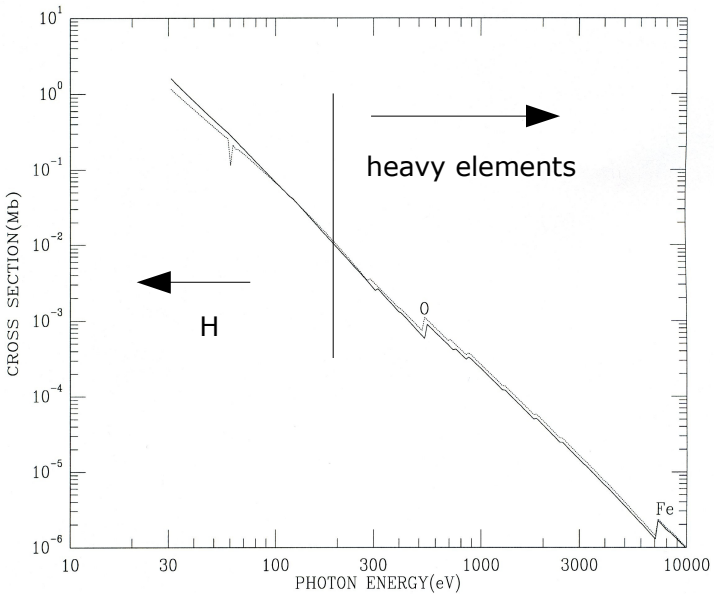

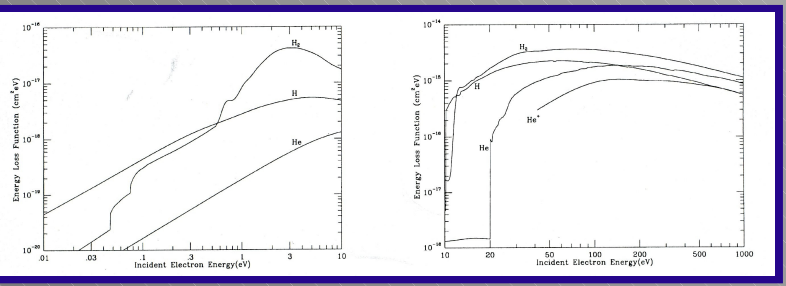

ELECTRON IMPACT

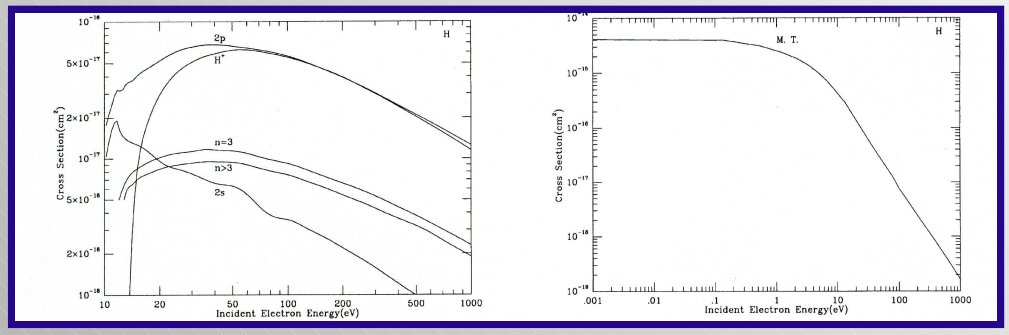

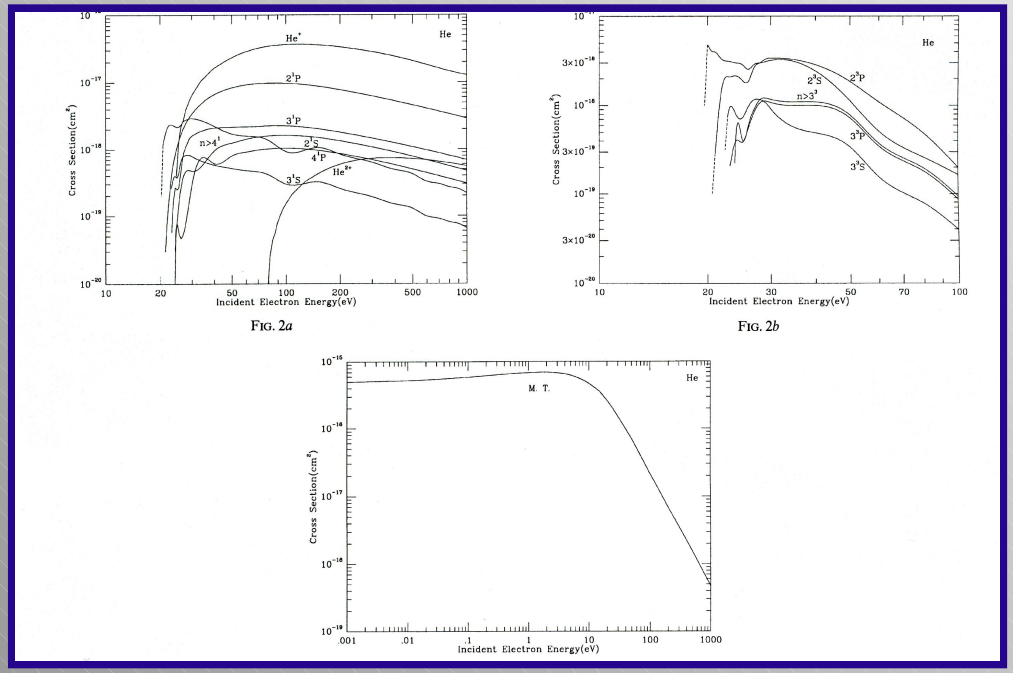

FIG. 2a

FIG. 2b

INPUT DATA: CROSS-SECTIONS

PHOTO-IONIZATION

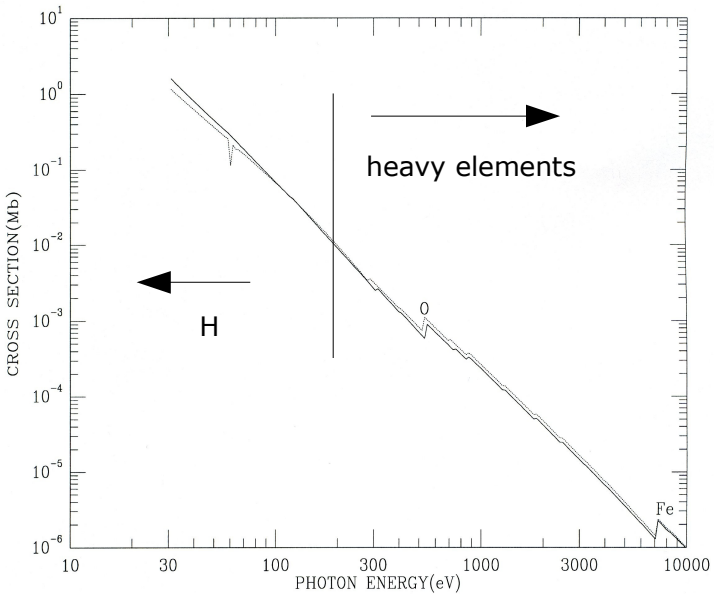

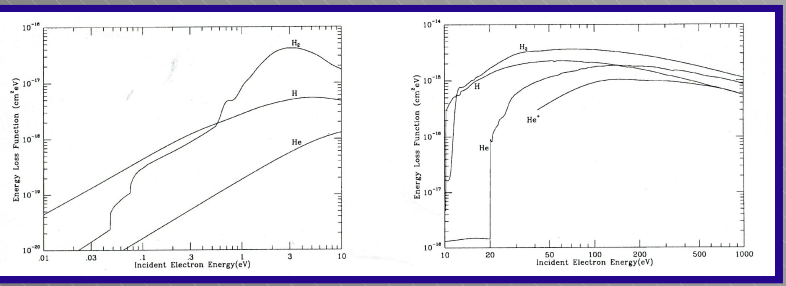

ELECTRON IMPACT

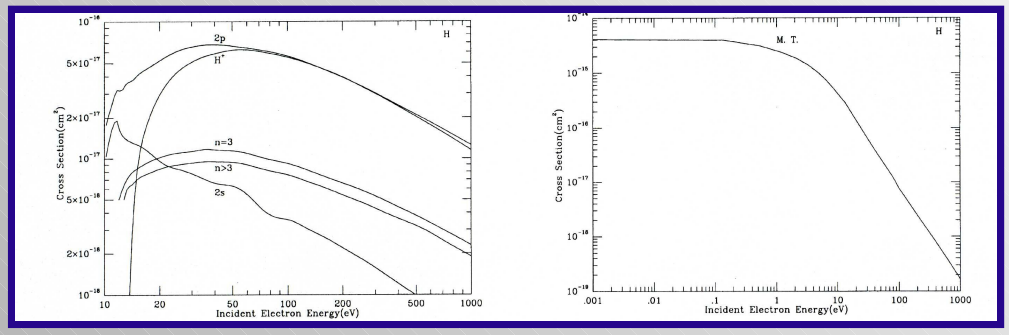

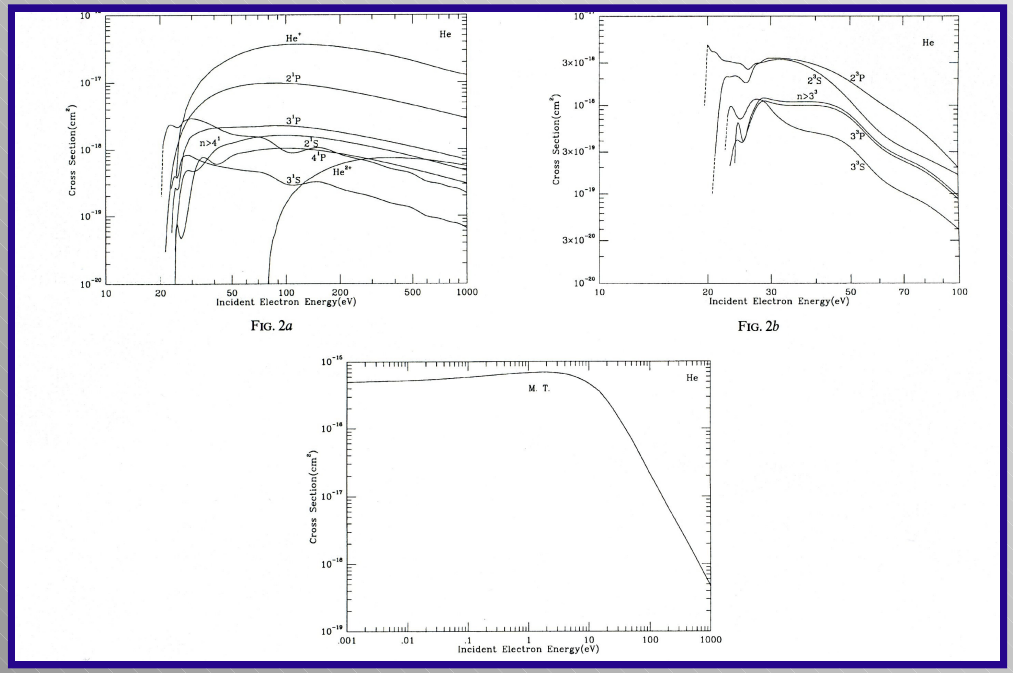

FIG. 2a

FIG. 2b

INPUT DATA: CROSS-SECTIONS

ELECTRON IMPACT

	discrete processes	ionization states	
H	4	1 (H^+)	+ elastic scattering
H_2	136	2 (H_2^+,H^-,H^+)	
He	12	2 (He^+,He^{2+})	

large data library → Dalgarno et al. (1999)

Remark: excitation cross-sections have considerable resonance structure not reproduced since the energy degradation process averages over them

OUTPUT DATA: MEAN ENERGY PER ION PAIR

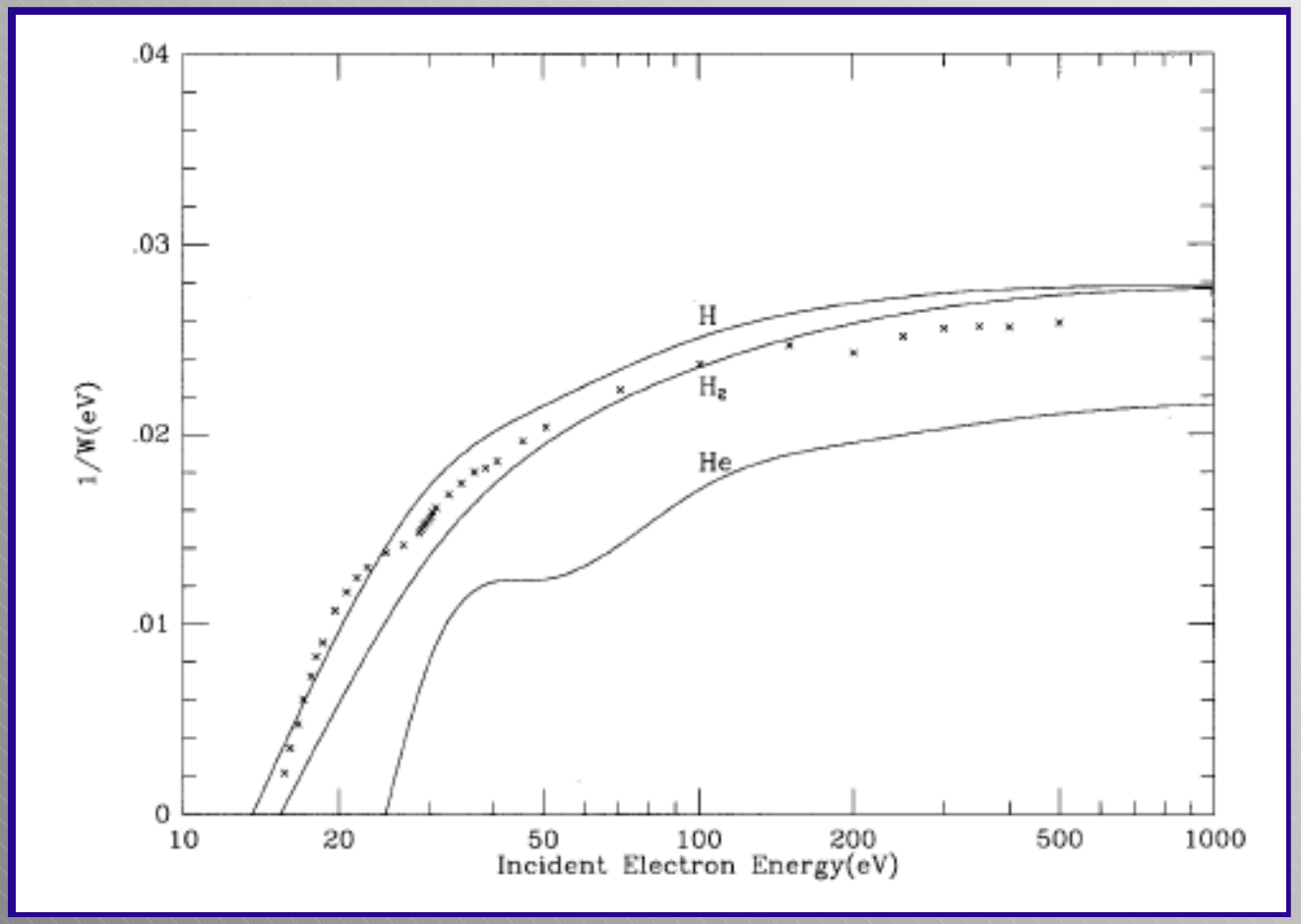

OUTPUT DATA: HEATING EFFICIENCY (per photo-electron)

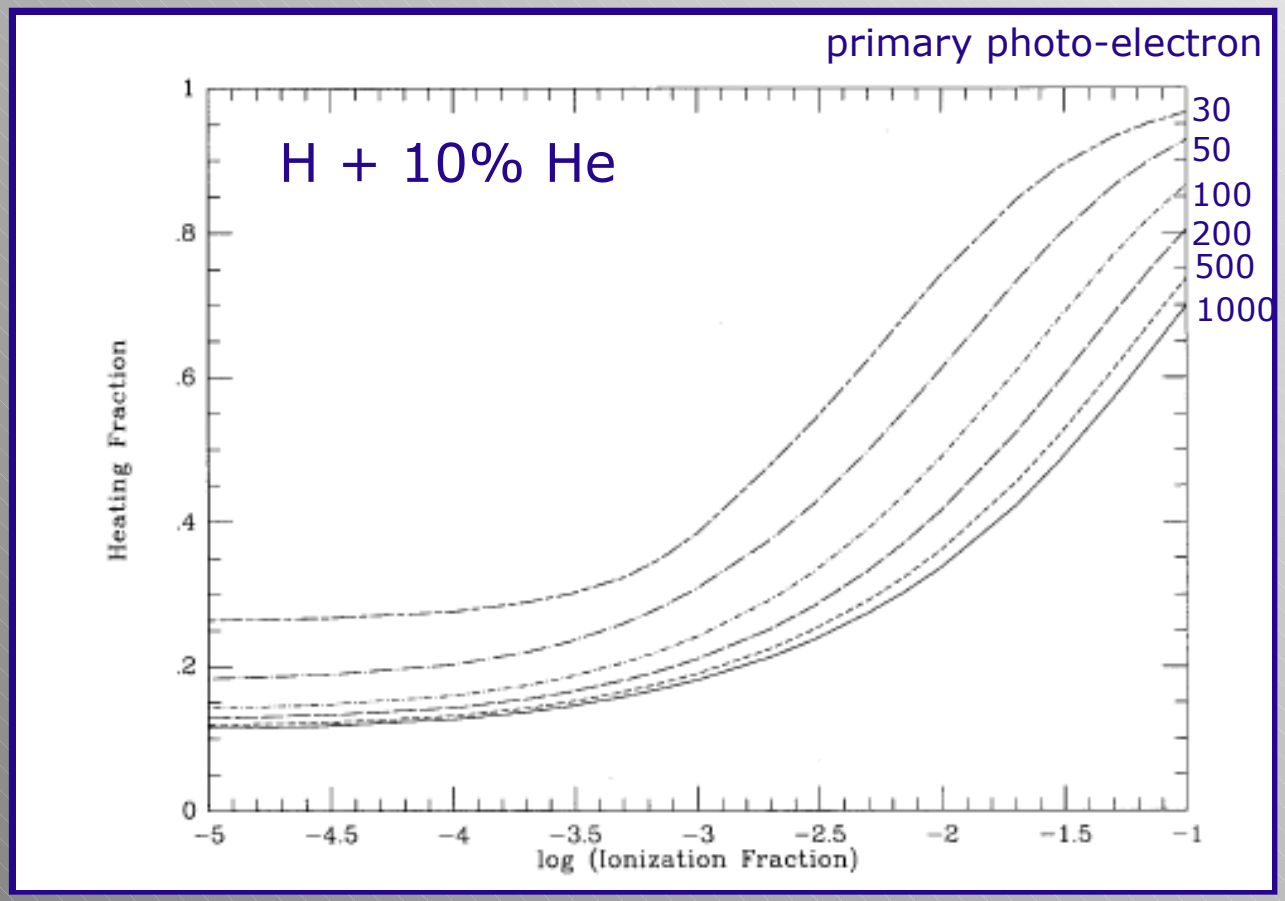

OUTPUT DATA: TRANSMITTED X-RAY FLUX

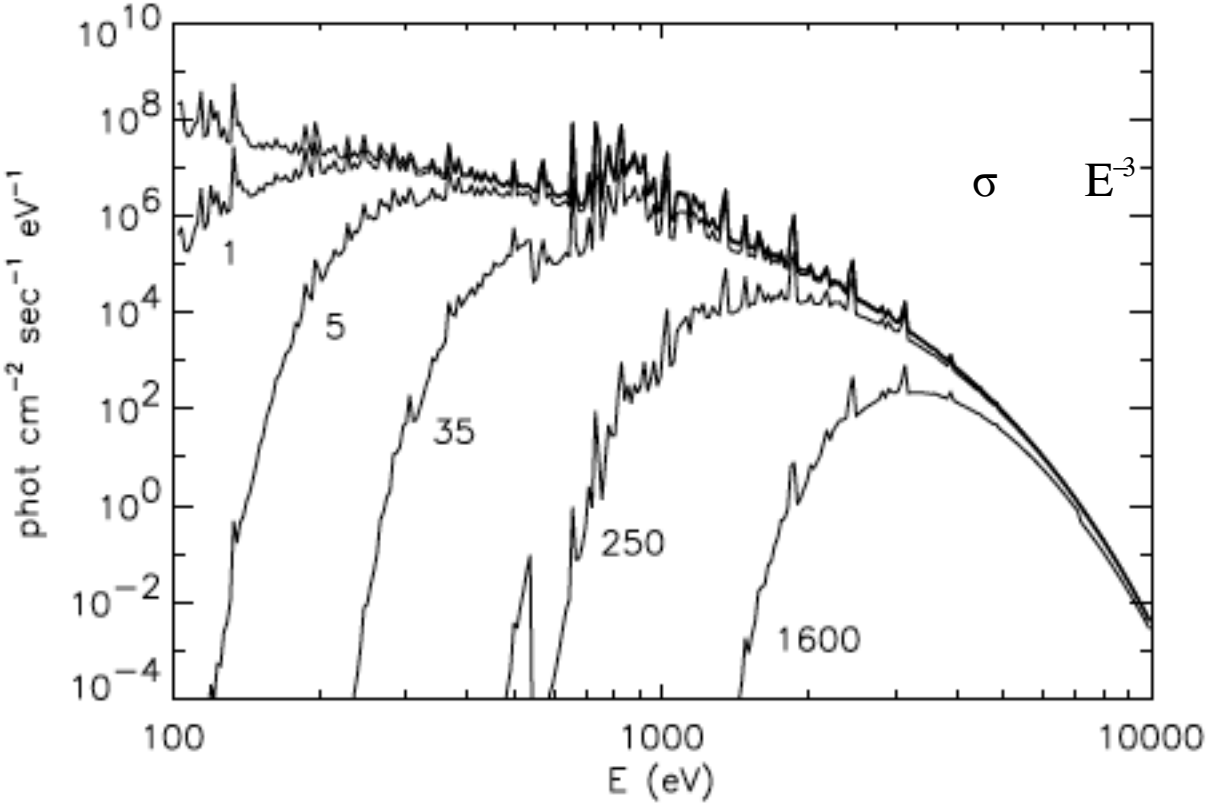

Fig. 1. Transmitted X-ray spectrum as a function of the energy at different of the atmospheric layers. The top curve is the incident stellar spectrum, obtained with a Raymond-Smith model at a temperature of 0.5 keV. **the spectrum becomes progressively weaker and harder**

SECONDARY PROCESSES

$$\zeta_1 = \int S_*(E)\left[\sigma_{\mathrm{pa}}(E) + \sigma_C\right] \mathrm{d}E$$

$$\zeta_T = f_{\mathrm{H}}\zeta_{\mathrm{H}} + f_{\mathrm{H_2}}\zeta_{\mathrm{H_2}} + f_{\mathrm{He}}\zeta_{\mathrm{He}}$$

$$\zeta_m = \int S_*(E)\left[\sigma_{\mathrm{pa}}(E)\,(E - I_m) + \sigma_C(E)\Delta E_C\right] \frac{\mathrm{d}E}{W_m(E)}$$

$$\frac{\mathrm{d}\mathcal{N}_1(E)}{\mathrm{d}E} = S_{XUV}(E + I_k, N_{\mathrm{H}}) \times \left[\sigma_{\mathrm{pa}}(E) + \sigma_C(E)\right]$$

$$Q_{XUV}(N_{\mathrm{H}}) = \sum_k \int \left(\frac{\mathrm{d}\mathcal{N}_1(E, N_{\mathrm{H}})}{\mathrm{d}E} \times \varepsilon_Q(E)\right)_k \mathrm{d}E.$$

1. RESULTS: MONOCHROMATIC FLUX

$$S^{\star}_{XUV} = S_0 \delta(E - E_0).$$

$S_0 = 1$

$$Q_{XUV}(N_{\rm H}) = S_0 \mathcal{E}_Q(E_0) \left[\sigma_{\rm pa}(E_0) + \sigma_C(E_0)\right] \times \exp\left[-\tau(N_{\rm H}, E_0)\right]$$

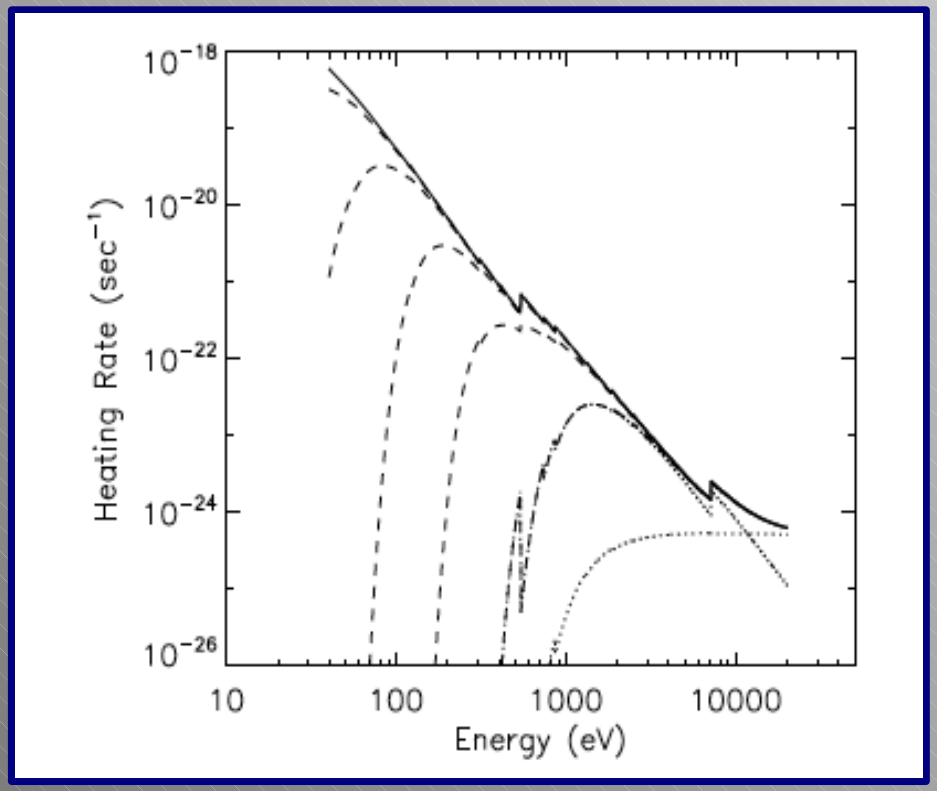

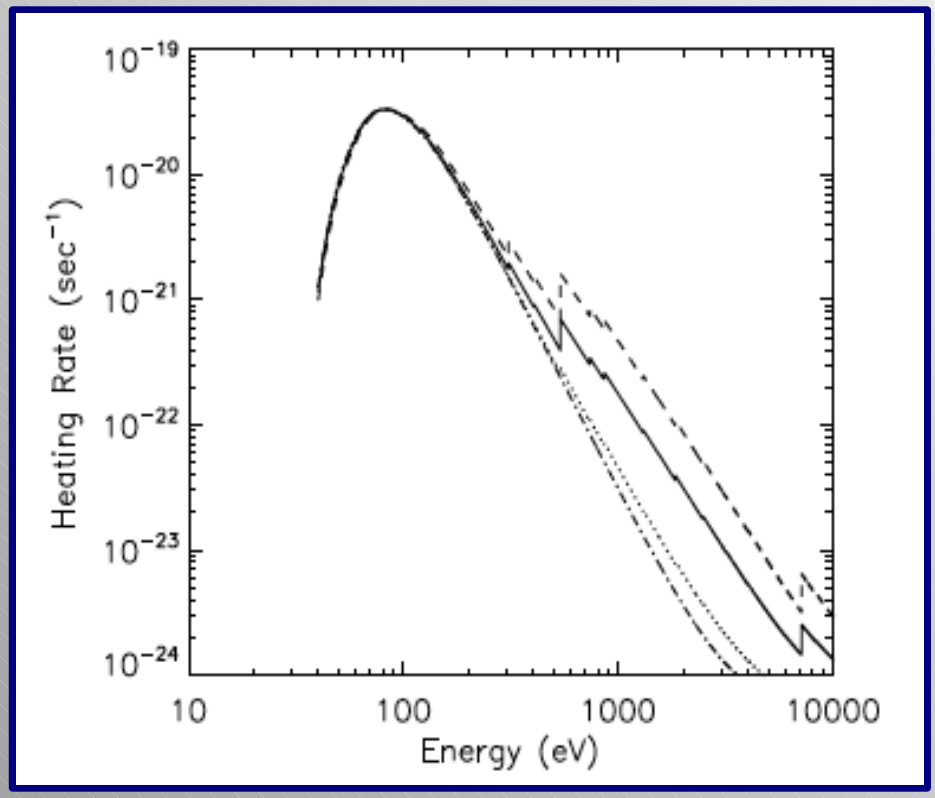

2. RESULTS: HEATING EFFICIENCY

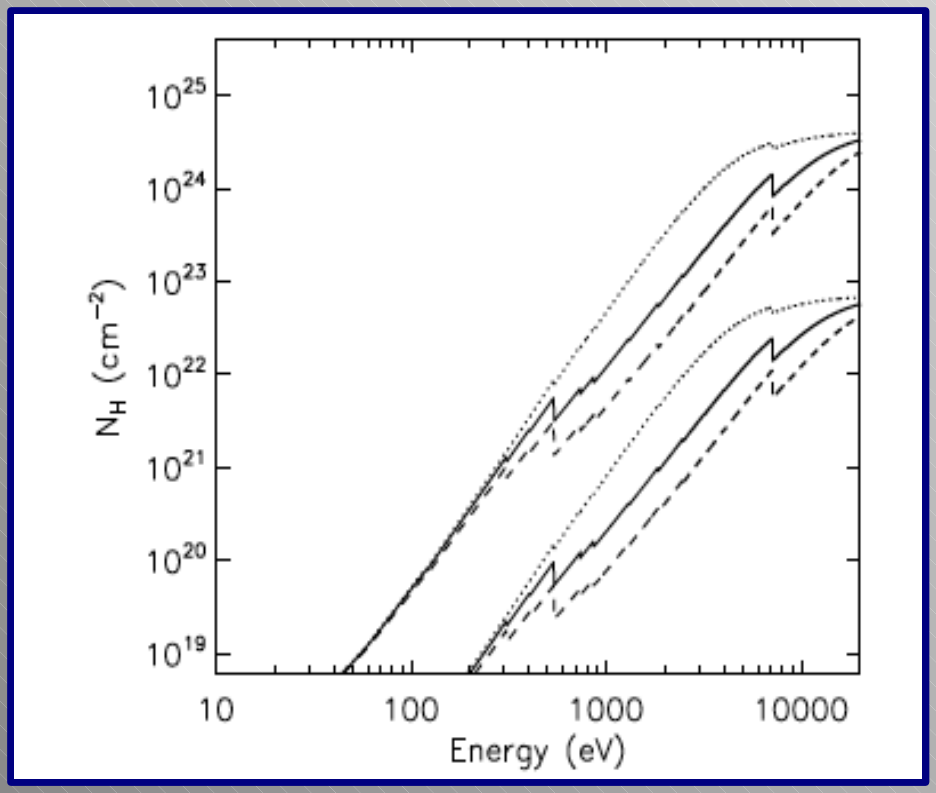

independent by the electron fraction

$$Y_Q = \left(\int S^{\star}_{\mathrm{XUV}}(E)\, \mathrm{d}E \right)^{-1} \times \int_0^{N_{\mathrm{H}}} Q_{\mathrm{XUV}}(N'_{\mathrm{H}})\, \mathrm{d}N'_{\mathrm{H}}.$$

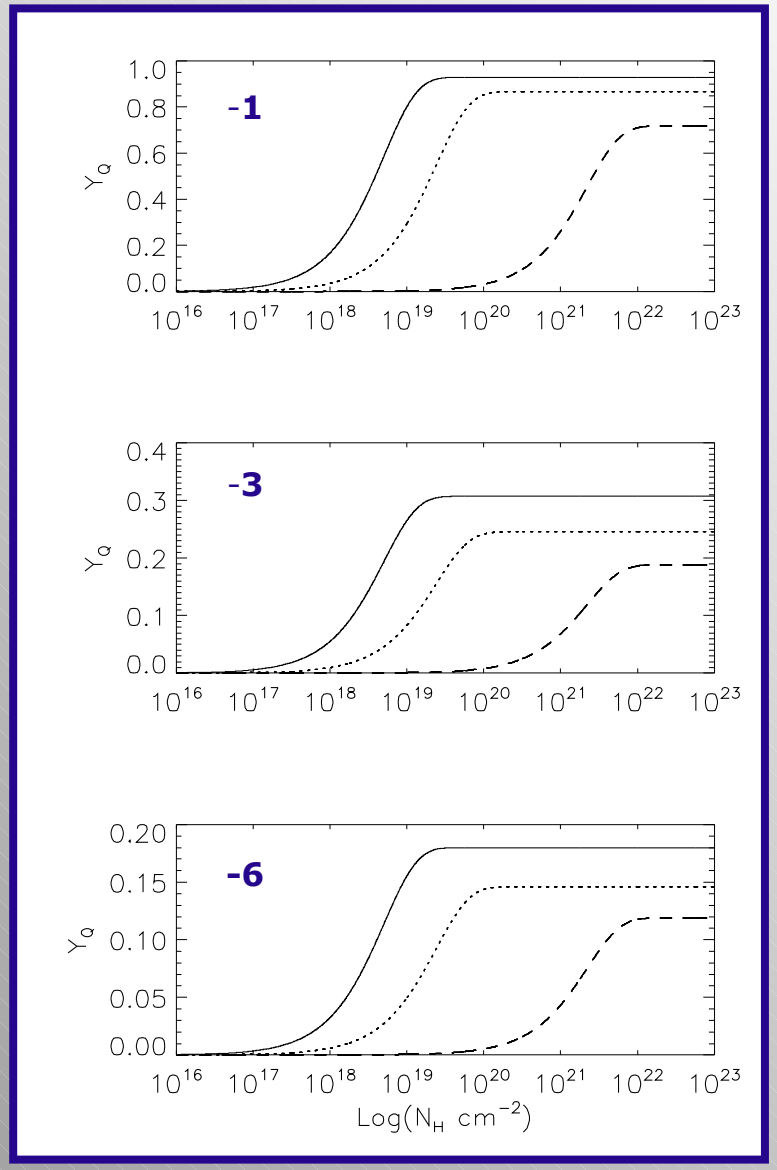

3. RESULTS: HD 209458b

It is one of most studied exoplanets (solar-like star HD 209458)

first

- transiting EP discovered
- EP known to have an atmosphere,
- EP observed to have an evaporating hydrogen atmosphere,
- EP found to have an atmosphere containing O and C
- EP to be directly observed spectroscopically
- EP found to have water vapour in its atmosphere

3. RESULTS: HD 209458b

$$n(R) = n_0 \exp\left[\frac{H}{R_P}\left(1 - \frac{R_P}{R}\right)\right]$$

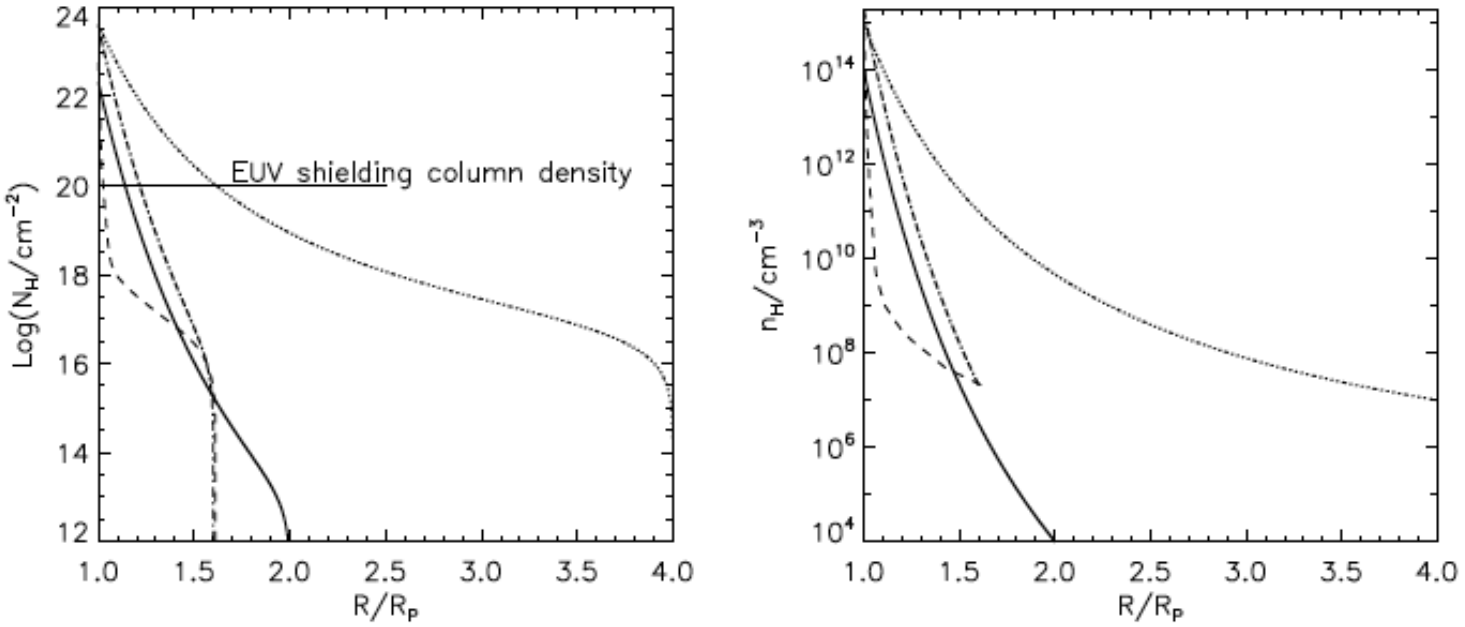

Fig. 5. Column density variation with the altitude inside atmospheres (*left panel*) whose density profiles (*right panel*) are described by Eq. (6). The solid line represents the model atmosphere with minimum total column density ($R_f = 2 \times R_P$, $n_0 = 1 \times 10^{14}$ cm^{-3}, $n(R_f) = 1 \times 10^4$ cm^{-3}) consistent with the assumed range of parameters (see text), while the dotted line represents the atmosphere with maximum total column density ($R_f = 4 \times R_P$, $n_0 = 1 \times 10^{15}$ cm^{-3}, $n(R_f) = 1 \times 10^7$ cm^{-3}). The case of the Yelle (2004) reference model for HD 209458b is shown for comparison as a dashed line; the dot-dashed curve is the equilibrium model obtained using the parameter set of values derived by Yelle (2004), i.e. $R_f = 1.6 \times R_P$, $n_0 = 2 \times 10^{15}$ cm^{-3}, $n(R_f) = 2 \times 10^7$ cm^{-3}.

4. RESULTS: STELLAR AGE

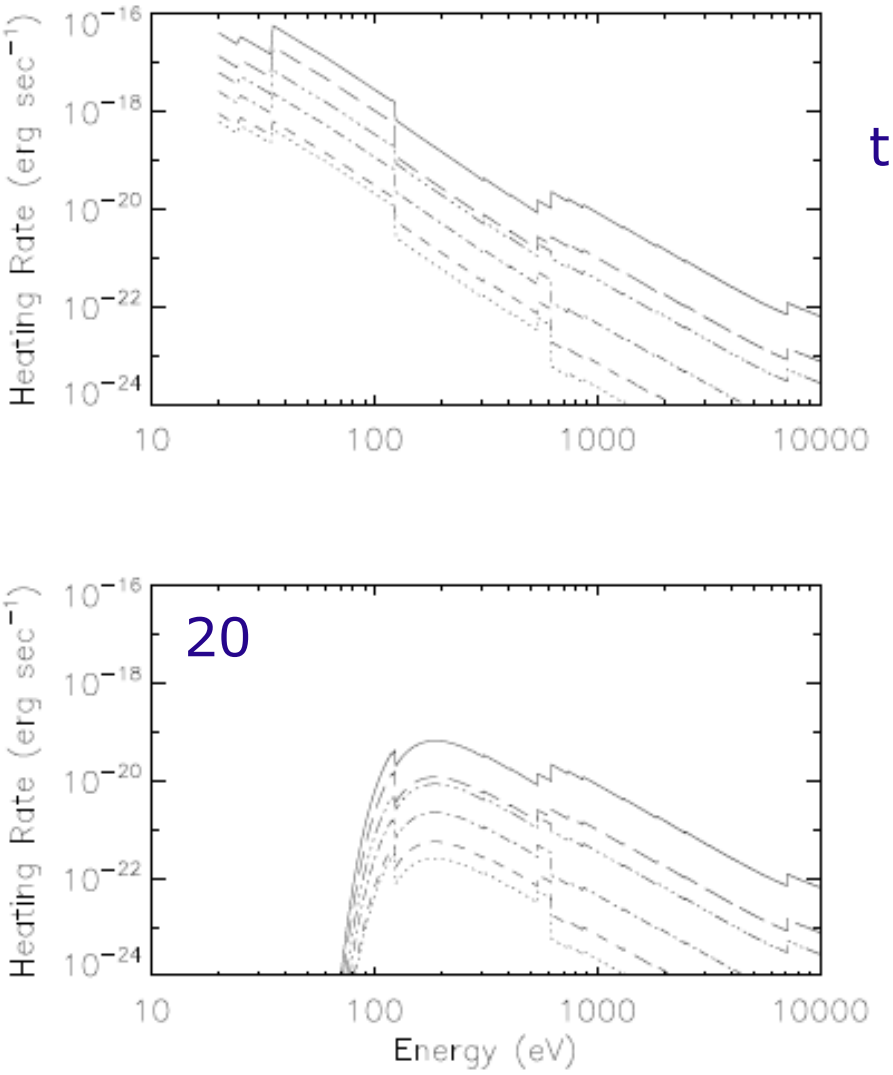

time

convolution

$Q_{XUV}(N_H, E_0) \otimes S^*(E)$

input flux (1 AU):

Ribas et al. 2005 ApJ

solar proxies:

ages from 0.1 to 6.7 Gyr